Nucleolin functions in nucleolus formation and chromosome congression

Nan Ma, Sachihiro Matsunaga, Hideaki Takata, Rika Ono-Maniwa, Susumu Uchiyama and Kiichi Fukui*

Department of Biotechnology, Graduate School of Engineering, Osaka University, 2-1 Yamadaoka, Suita 565-0871, Osaka, Japan
*Author for correspondence (e-mail: kfukui@bio.eng.osaka-u.ac.jp)

Accepted 17 April 2007
Journal of Cell Science 120, 2091-2105 Published by The Company of Biologists 2007
doi:10.1242/jcs.008771

Summary

A complex structure, designated the chromosome periphery, surrounds each chromosome during mitosis. Although several proteins have been shown to localize to the chromosome periphery, their functions during mitosis remain unclear. Here, we used a combination of high-resolution microscopy and RNA-interference-mediated depletion to study the functions of nucleolin, a nucleolar protein localized at the chromosome periphery, in interphase and mitosis. During mitosis, nucleolin was localized in the peripheral region including the vicinity of the outer kinetochore of chromosomes. Staining with an antibody specific for nucleolin phosphorylated by CDC2 revealed that nucleolin was also associated with the spindle poles from prometaphase to anaphase. Nucleolin depletion resulted in disorganization of the nucleoli at interphase. Furthermore, nucleolin-depleted cells showed a prolonged cell cycle with misaligned chromosomes and defects in spindle organization. The misaligned chromosomes showed syntelic kinetochore-microtubule attachments with reduced centromere stretching. Taken together, our results indicate that nucleolin is required for nucleolus formation, and is also involved in chromosome congression and spindle formation.

Key words: Nucleolin, Nucleolus formation, Chromosome congression, Mitosis

Introduction

A layer around chromosomes during mitosis was first observed by light microscopy about 80 years ago (Sharp, 1929), and subsequent electron microscopic studies revealed a layer of closely packed fibrils and dense granules around each chromosome (Gautier et al., 1992a; Gautier et al., 1992b). The layer, designated the 'chromosome periphery' (Hernandez-Verdun and Gautier, 1994), appears at prometaphase and disappears at telophase during mitosis. It contains numerous components, including nuclear and nucleolar proteins as well as several RNAs (Van Hooser et al., 2005).

Some nucleolar proteins were found to bind to the surface of chromosomes throughout mitosis, and then become incorporated into the newly formed nucleoli at the end of telophase (Azum-Gélade et al., 1994; Dundr et al., 1997). Therefore, the chromosome, and especially its periphery, has been proposed to act as a means of transport for various proteins, including nucleolar proteins. Besides its transportation function, the chromosome periphery may also play active roles in chromosome structure. As an example, the chromosome peripheral protein Ki-67 is involved in the formation of higher-order chromatin structures (Takagi et al., 1999; Kametaka et al., 2002; Scholzen et al., 2002; Saiwaki et al., 2005). In addition, it has been speculated that the chromosome periphery is involved in the progression of mitosis, possibly by participating in the protection and stabilization of the chromosomes. An example for this scenario is the chromosome peripheral protein complex Ku, which appears to protect chromosome telomeres (Bertuch and Lundblad, 2003).

In our recent proteome analysis, 107 proteins were identified in highly purified human metaphase chromosomes (Uchiyama et al., 2005). Furthermore, the observation that more than a quarter of the identified proteins were classified as chromosome peripheral proteins strongly suggests that these proteins are related to either chromosome organization or mitotic progression. Human nucleolin, a 710 amino acid protein, is one of the major and most extensively studied nucleolar proteins. An analysis of its amino acid sequence revealed the presence of three different structural domains, the N-terminal, central and C-terminal domains (Ginisty et al., 1999). The N-terminal domain is composed of highly acidic regions and contains multiple phosphorylation sites. The central domain contains four RNA-binding domains. The C-terminal domain is rich in glycine, arginine and phenylalanine residues. Nucleolin is highly conserved in many eukaryotic species. Proteins with homology to human nucleolin have been identified in *Saccharomyces pombe* (Gulli et al., 1995), *Xenopus laevis* (Caizergues-Ferrer et al., 1989), *Arabidopsis thaliana* (Didier and Klee, 1992) and peas (Tong et al., 1997).

The nucleolus is the site responsible for ribosome biogenesis (Hernandez-Verdun, 2005). As visualized by electron microscopy, the nucleolus consists of three main components, designated fibrillar centers (FCs), dense fibrillar components (DFCs) and granular components (GCs). The relatively opaque FCs in mammalian nucleoli are surrounded by the highly contrasted fine strands of DFCs. In turn, the DFCs are surrounded by GCs, which fill out the peripheral parts of the nucleolus. Subsequent studies revealed that the FCs harbor copies of rRNA genes, and it is well established that the initial pre-rRNA resides in the DFCs, whereas late processing events take place in the GCs. Finally, pre-ribosomal particles are translocated to the cytoplasm (Shaw and Doonan, 2005).

Nucleolin is an abundant nucleolar protein localized in the DFCs and GCs of nucleoli (Biqqioqera et al., 1990). Nucleolin plays essential roles in rDNA transcription, rRNA maturation, ribosome assembly and nucleocytoplasmic transport (Ginisty et al., 1999; Srivastava and Pollard, 1999). As a multifunctional protein, nucleolin has also been proposed to be a nuclear matrix-binding protein (Gotzmann et al., 1997), to interact with telomerase (Khurts et al., 2004) and to be involved in the regulation of apoptosis (Mi et al., 2003), intestinal cell differentiation (Turck et al., 2006) and remodeling of nucleosomes (Angelov et al., 2006). Although many functions of nucleolin have been clarified, previous studies have fallen short of demonstrating its functions during mitosis.

Nucleolin is highly phosphorylated (Olson et al., 1975; Rao et al., 1982) and its phosphorylation is highly regulated during the cell cycle (Peter et al., 1990; Morimoto et al., 2005). Extensive phosphorylation by casein kinase 2 (CK2) occurs at interphase and by CDC2 during mitosis (Peter et al., 1990), and this regulated phosphorylation of nucleolin probably regulates nucleolin functions during the cell cycle (Ginisty et al., 1999). It has been demonstrated that phosphorylation of nucleolin at interphase is correlated with active rRNA transcription (Suzuki et al., 1987). Despite a previous study describing the localization of nucleolin phosphorylated by CDC2 (Dranovsky et al., 2001), no information about its functions during mitosis has been obtained to date.

Here, we demonstrate that nucleolin localizes to the nucleoli, which are located in the peripheral region including the vicinity of the outer kinetochore of chromosomes, in interphase nuclei and during mitosis. Staining with an antibody specific for nucleolin phosphorylated by CDC2 reveals that nucleolin is also associated with the spindle poles from prometaphase to anaphase. Using the RNA interference (RNAi) technique, cells depleted of nucleolin show disorganization of the nucleoli accompanied by loss of the nucleolar proteins fibrillarin, B23 and Ki-67. The main finding of this study is disruption of chromosome congression in cells depleted of nucleolin. We show that this defect is due to improper kinetochore attachments, resulting in reduced tension, and syntelic attachments. Depletion of nucleolin also appears to affect spindle assembly.

Results

Localization analyses of nucleolin

Although the localization of nucleolin has previously been described (Azum-Gélade et al., 1994; Medina et al., 1995; Dundr et al., 1997; Gotzmann et al., 1997; Piñol-Roma, 1999), its dynamic localization during the cell cycle has not been reported. To investigate this, immunostaining for nucleolin was examined throughout the cell cycle (Fig. 1A). At interphase, nucleolin was prominently localized at the outer layer of the nucleoli, and present at a lower concentration throughout the nucleoplasm. At prophase, most of the nucleolin remained in the nucleolar remnants. When the nuclear membrane and nucleoli were disrupted at prometaphase, nucleolin began to disperse throughout the cytoplasm and localize at the chromosome periphery. At metaphase, nucleolin was localized at the chromosome periphery and slightly distributed in the cytoplasm. At anaphase, some nucleolin remained associated with the chromosome periphery, while some became packaged into cytoplasmic particles known as nucleolus-derived foci (NDFs) (Dundr et al., 1997). At telophase I (early telophase), nucleolin was still associated with chromosomes, and a fraction of it accumulated into NDFs and pre-nucleolar bodies (PNBs) (Dundr et al., 1997). The NDFs disappeared at telophase II (late telophase) and were replaced by PNBs.

Nucleolin was evenly detected in the chromosome periphery in metaphase chromosome spreads (Fig. 1B). It was also detected between the two chromatids of each chromosome and in the kinetochores. The detailed localization of nucleolin in the kinetochore was clarified by staining with an antibody against aurora kinase B (Aurora-B) as a centromeric heterochromatin marker, the anti-centromere autoimmune serum (CREST) as an inner kinetochore marker and an antibody against Mad2 as an outer kinetochore marker. Interestingly, the signals for nucleolin were separate from those for Aurora-B or CREST, but adjacent to those for Mad2, suggesting that nucleolin is localized in the vicinity of the outer kinetochore. When fibrillarin, another chromosome peripheral protein, was double-stained with nucleolin in metaphase chromosome spreads, the two proteins overlapped in the chromosome periphery and were colocalized in the vicinity of the outer kinetochore. The localization of nucleolin in the vicinity of the outer kinetochore was confirmed by line scans through kinetochore pairs (Fig. 1C), and by measuring the distances between the centers of the immunofluorescence signals for nucleolin and those for Aurora-B, CREST, Mad2 and fibrillarin (Fig. 1D).

Nucleolin is required for nucleolus formation

We depleted human nucleolin in HeLa cells by using RNAi. A nonspecific small interference RNA (siRNA) was used for control transfections. Two different siRNA oligonucleotides (siRNA1 and siRNA2) were used to exclude any potential off-target effects of the RNAi. The cellular expression levels of nucleolin were reduced to 15.5% and 39.1% after transfection with siRNA1 and siRNA2, respectively (Fig. 2A). No significant reductions in the expression levels of fibrillarin, B23, β-actin and α-tubulin were detected. These data are consistent with a recent report that depletion of nucleolin by siRNA did not considerably affect the expression levels of other proteins, including B23, aprataxin and β-tubulin (Becherel et al., 2006). To further increase our confidence in the data obtained from the siRNA experiments, we checked the expression levels of several proteins, including cyclin B1 and hnRNP-U in total cell extracts, and CDC20, CDC27 (a subunit of the anaphase-promoting complex), Aurora-B, BubR1 and Hec1 (one of the subunits of human NDC80 complex) in mitotic cell extracts. The results revealed that the expression levels of these proteins were not considerably affected by nucleolin RNAi (data not shown). RNAi-mediated depletion of nucleolin resulted in dramatic reductions in its fluorescence intensities in both the nucleoli and chromosome periphery (Fig. 2B). For siRNA1 depletion, the average intensities of nucleolin in the nucleoli and chromosome periphery were decreased by 66.2±7.8% and 73.3±7.0%, respectively, compared with the values in control cells. For siRNA2 depletion, the average intensities of nucleolin in the nucleoli and chromosome periphery were decreased by 59.1±7.4% and 63.1±8.6%, respectively, compared with the values in control cells.

To compare the localization of nucleolin with those of other nucleolar proteins, two different DFC markers, namely

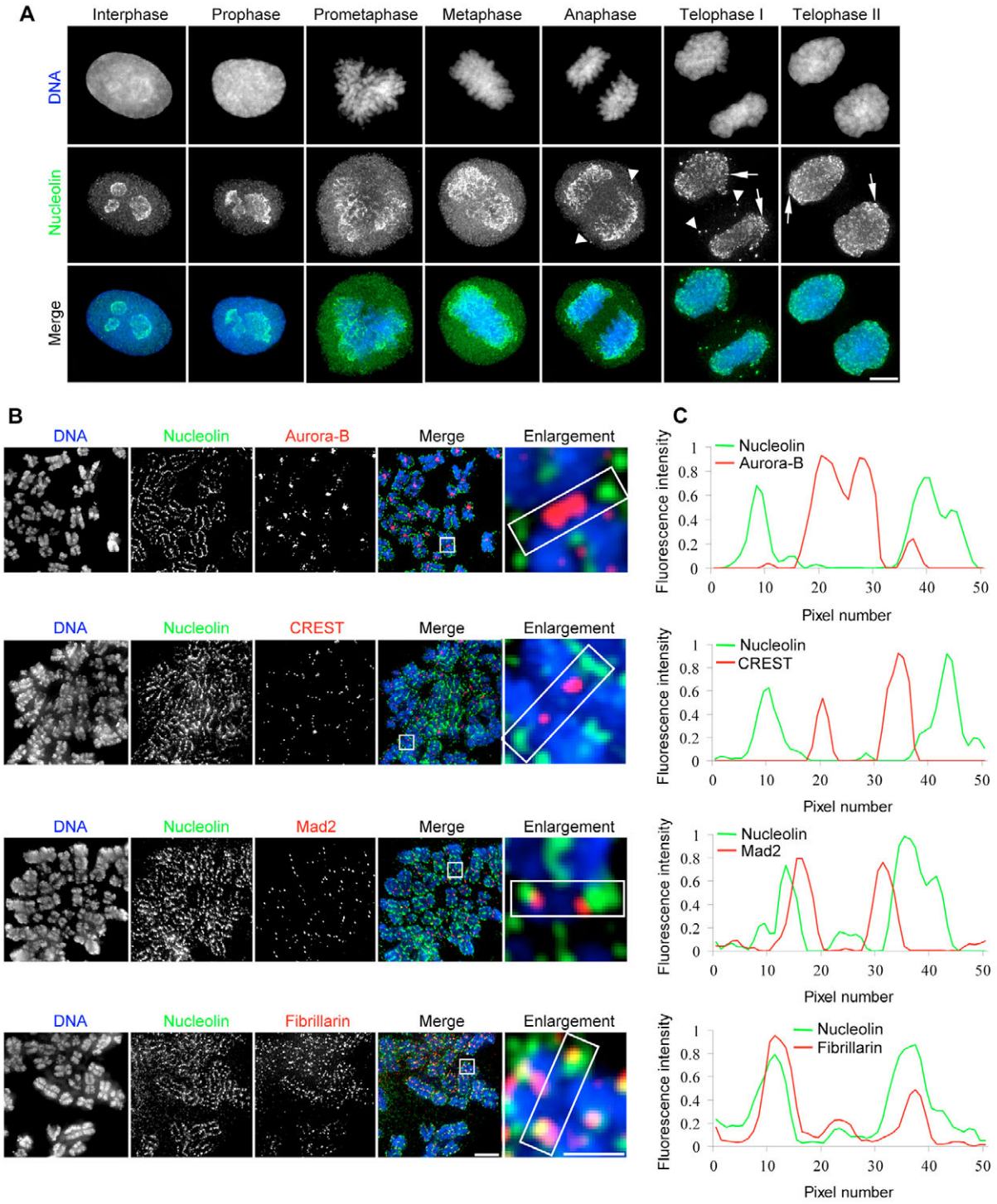

Fig. 1. Dynamic localization of nucleolin during the cell cycle. (A) HeLa cells were stained for nucleolin (green) at different phases of the cell cycle. Arrowheads indicate NDFs, arrows show PNBs. (B) Metaphase chromosome spreads stained with nucleolin (green), Aurora-B (red), CREST (red), Mad2 (red) and fibrillarin (red) antibodies. Enlargements show examples of the centromeric regions. The rectangles indicate the planes where the line scans in C were performed. (C) Corresponding fluorescence intensity profiles of line scans. (D) Measurements of the distances between the centers of immunofluorescence signals for nucleolin and those for Aurora-B, CREST, Mad2 and fibrillarin. More than 50 kinetochores were measured in each experiment. Bars, 5 μm; 1.25 μm (Enlargement).

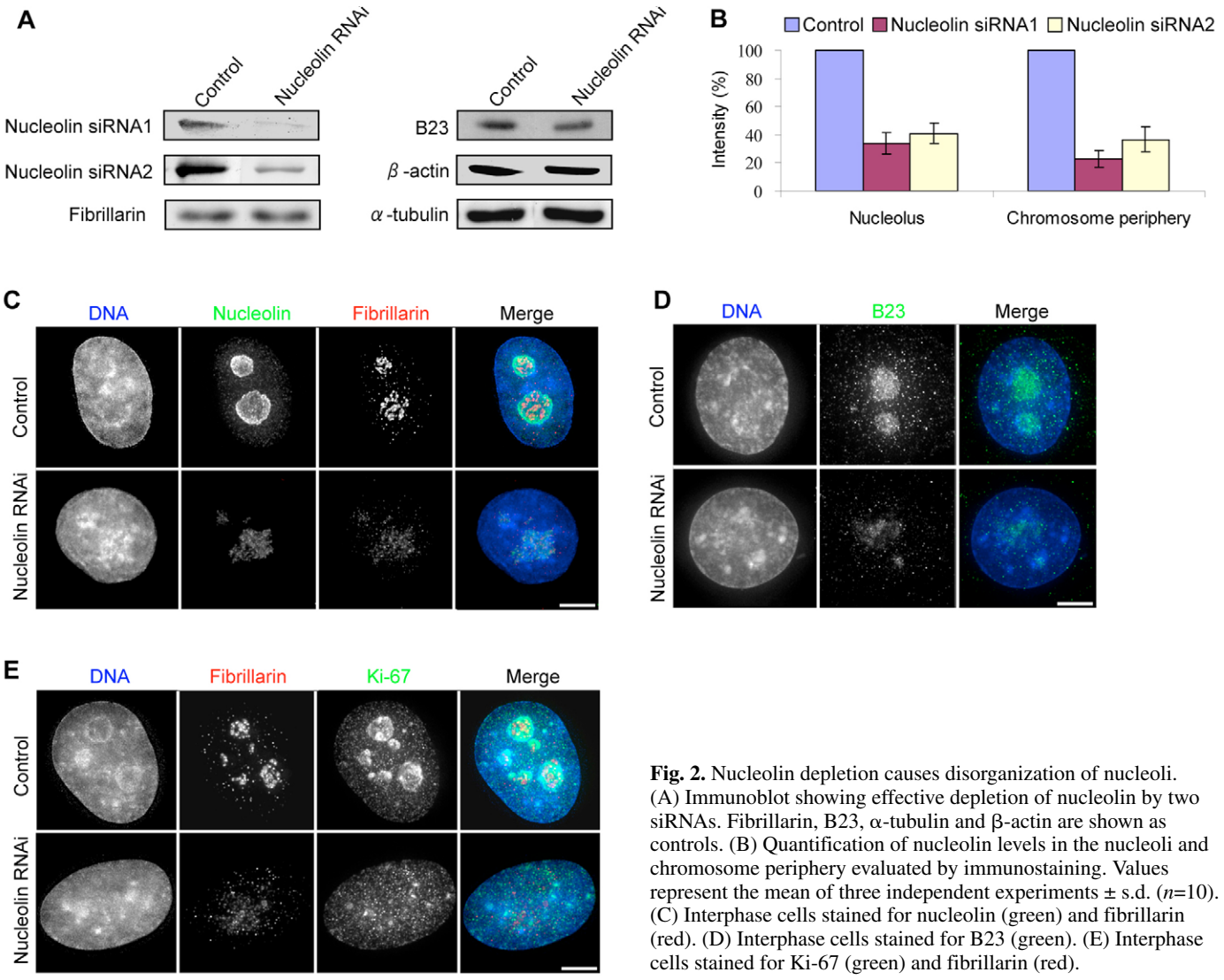

Fig. 2. Nucleolin depletion causes disorganization of nucleoli. (A) Immunoblot showing effective depletion of nucleolin by two siRNAs. Fibrillarin, B23, α-tubulin and β-actin are shown as controls. (B) Quantification of nucleolin levels in the nucleoli and chromosome periphery evaluated by immunostaining. Values represent the mean of three independent experiments ± s.d. (n=10). (C) Interphase cells stained for nucleolin (green) and fibrillarin (red). (D) Interphase cells stained for B23 (green). (E) Interphase cells stained for Ki-67 (green) and fibrillarin (red).

fibrillarin (Fomproix et al., 1998) and Ki-67 (Kill, 1996), and one marker for both DFCs and GCs, namely B23 (Biqqioqera et al., 1990), were stained in the nucleoli. Nucleolin was mainly localized at the outer layer with fainter staining at the center of the nucleoli (Fig. 2C). By contrast, fibrillarin appeared as discrete dot-like foci within the nucleoli. B23 was almost uniformly dispersed over the whole nucleoli (Fig. 2D). In a previous study, Ki-67 was detected in large numbers of discrete foci throughout the nucleoplasm during early G1 (Kill, 1996). In the present study, Ki-67 was localized in the nucleoli during S and G2 phase (Fig. 2E), consistent with that previous study (Kill, 1996). In cells depleted by siRNAs targeting nucleolin, the spherical shape of the nucleoli became irregular, as revealed by the weak nucleolar staining of nucleolin, fibrillarin and B23 (Fig. 2C,D). In the nucleolin-depleted cells, Ki-67 was dispersed throughout the nuclei without any obvious staining in the nucleoli (Fig. 2E). After nucleolin depletion, the relative fluorescence intensity of nucleolin in the nucleoli was considerably reduced (Fig. 2B). Unexpectedly, the average intensities of several other nucleolar proteins, including fibrillarin, B23 and Ki-67, in the nucleolin-depleted nucleoli were decreased by 69.4%, 30.9% and 68.1% compared with the corresponding values in control cells. These fluorescence reductions were probably due to dispersion of fibrillarin and B23 by nucleolin RNAi, although the expression levels of these two proteins were not considerably changed (Fig. 2A). These data suggest that nucleolin is responsible for maintaining the shape and functional compartmentalization of nucleoli, since the spherical structures of the nucleoli and DFCs, which were marked by fibrillarin or Ki-67 staining, were highly disorganized.

Nucleolin depletion activates the spindle checkpoint

During mitosis, nucleolin depletion induced the accumulation of mitotic cells. The mitotic index of nucleolin-depleted cells was approximately two-fold higher in cells after RNAi with siRNA1 (5.7±0.4%) than in control cells (2.7±0.2%) at 72 hours after transfection (Fig. 3A). Similar effects were seen in the samples transfected with siRNA2. Upon depletion of Aurora-B by RNAi, checkpoint proteins, including BubR1 and Mad2, are rarely recruited to the kinetochores and the spindle checkpoint is silenced, triggering mitotic exit (Vagnarelli and

Earnshaw, 2004). To determine whether the spindle checkpoint can be activated in nucleolin-depleted cells, we used siRNAs to deplete nucleolin alone or nucleolin and Aurora-B simultaneously. Using immunostaining and immunoblotting, we confirmed that both proteins were depleted to the same levels as those observed for the single siRNA treatments (data not shown). In cells only depleted of nucleolin, the mitotic index increased considerably compared with that in control

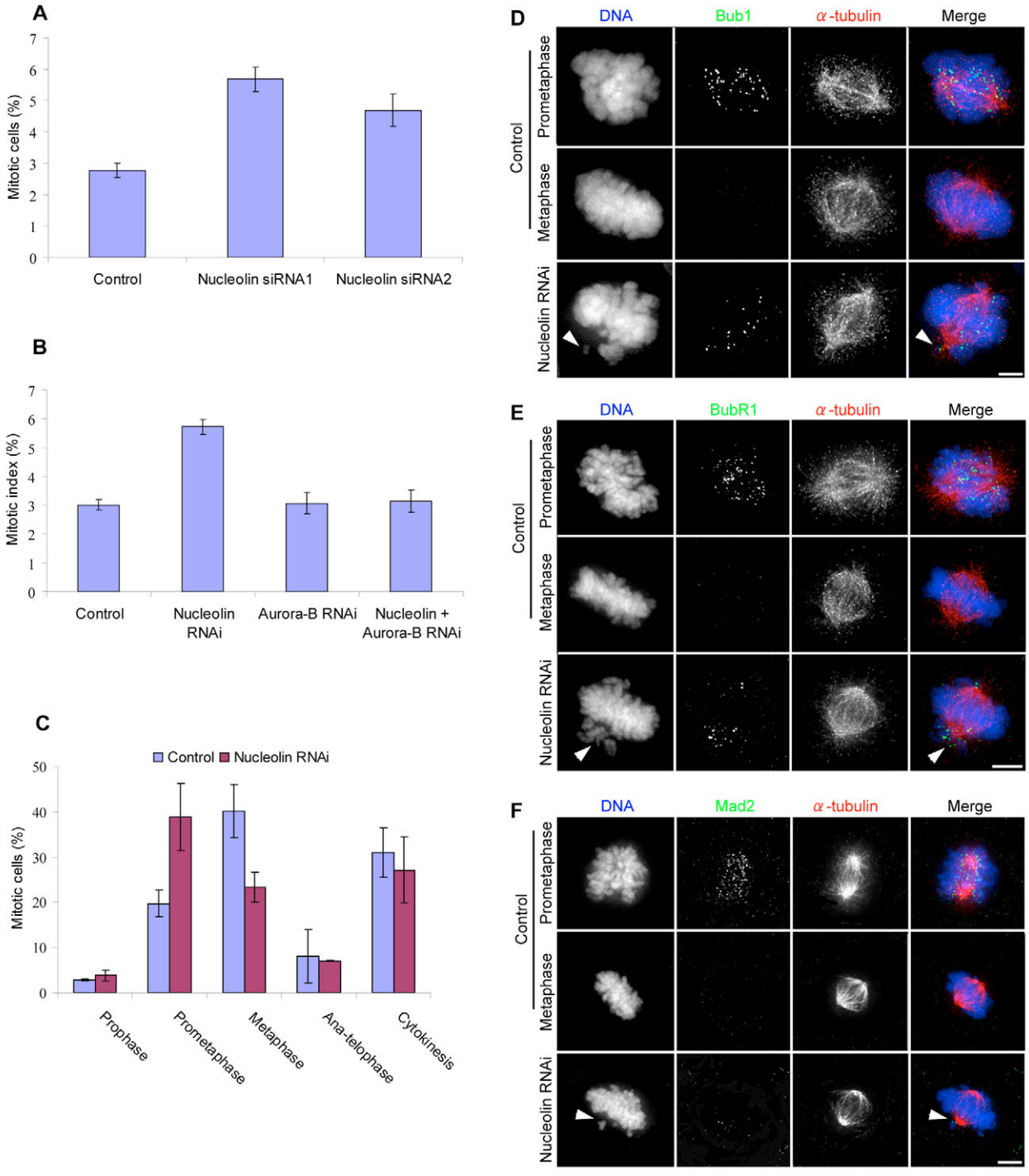

Fig. 3. Nucleolin depletion induces spindle-checkpoint activation. (A) Mitotic indexes of control cells and cells depleted of nucleolin by siRNA1 or siRNA2. Values represent the mean of three independent experiments ± s.d. (n=400). (B) Mitotic indexes of control, nucleolin-depleted, Aurora-B-depleted and both nucleolin- and Aurora-B-depleted cells at 72 hours after control and RNAi transfections. Values represent the means of three independent experiments ± s.d. (n=400). (C) Percentages of control and nucleolin-depleted cells at different stages in the cell cycle. Values represent the mean of four independent experiments ± s.d. (n=400). (D) Mitotic cells stained for Bub1 (green) and α-tubulin (red). (E) Mitotic cells stained for BubR1 (green) and α-tubulin (red). (F) Mitotic cells stained for Mad2 (green) and α-tubulin (red). Arrowheads in D,E and F show misaligned chromosomes and the fluorescence signals for Bub1, BubR1 and Mad2 at the kinetochores, respectively. Bars, 5 μm.

cells (Fig. 3B). However, in cells simultaneously depleted of both nucleolin and Aurora-B, the mitotic index was similar to that in control cells, suggesting that the mitotic delay observed in nucleolin-depleted cells resulted from spindle-checkpoint activation. Consistent with our hypothesis, quantification of the distinct mitotic stages revealed that the nucleolin-depleted cells showed a two-fold increase in the population of prometaphase cells (Fig. 3C). To further confirm this finding, the spindle-checkpoint proteins Bub1, BubR1 or Mad2 were double-stained with α-tubulin in control and nucleolin-depleted cells. At prometaphase, the three spindle checkpoint proteins were recruited to the kinetochores in control cells (Fig. 3D-F). When the cells proceeded to metaphase, Bub1, BubR1 and Mad2 showed either a lack of association with the kinetochores of aligned chromosomes or were present at low levels (Fig. 3D-F). In nucleolin-depleted cells, Bub1, BubR1 and Mad2 were detected at the kinetochores of misaligned chromosomes, but not at those of chromosomes aligned at the spindle equator (Fig. 3D-F). Taken together, these data suggest that nucleolin depletion activates the spindle checkpoint.

Nucleolin is involved in chromosome congression

After incubation with the siRNAs targeting nucleolin, signals for nucleolin were rarely detected in mitotic cells (Fig. 2B, Fig. 4A) or chromosome metaphase spreads (Fig. 4B). Interestingly, signals for both fibrillarin (Fig. 4B) and B23 (data not shown) in the chromosome periphery also disappeared after nucleolin depletion. Nucleolin depletion mainly induced two types of pronounced defects in chromosome congression: misalignment and non-alignment.

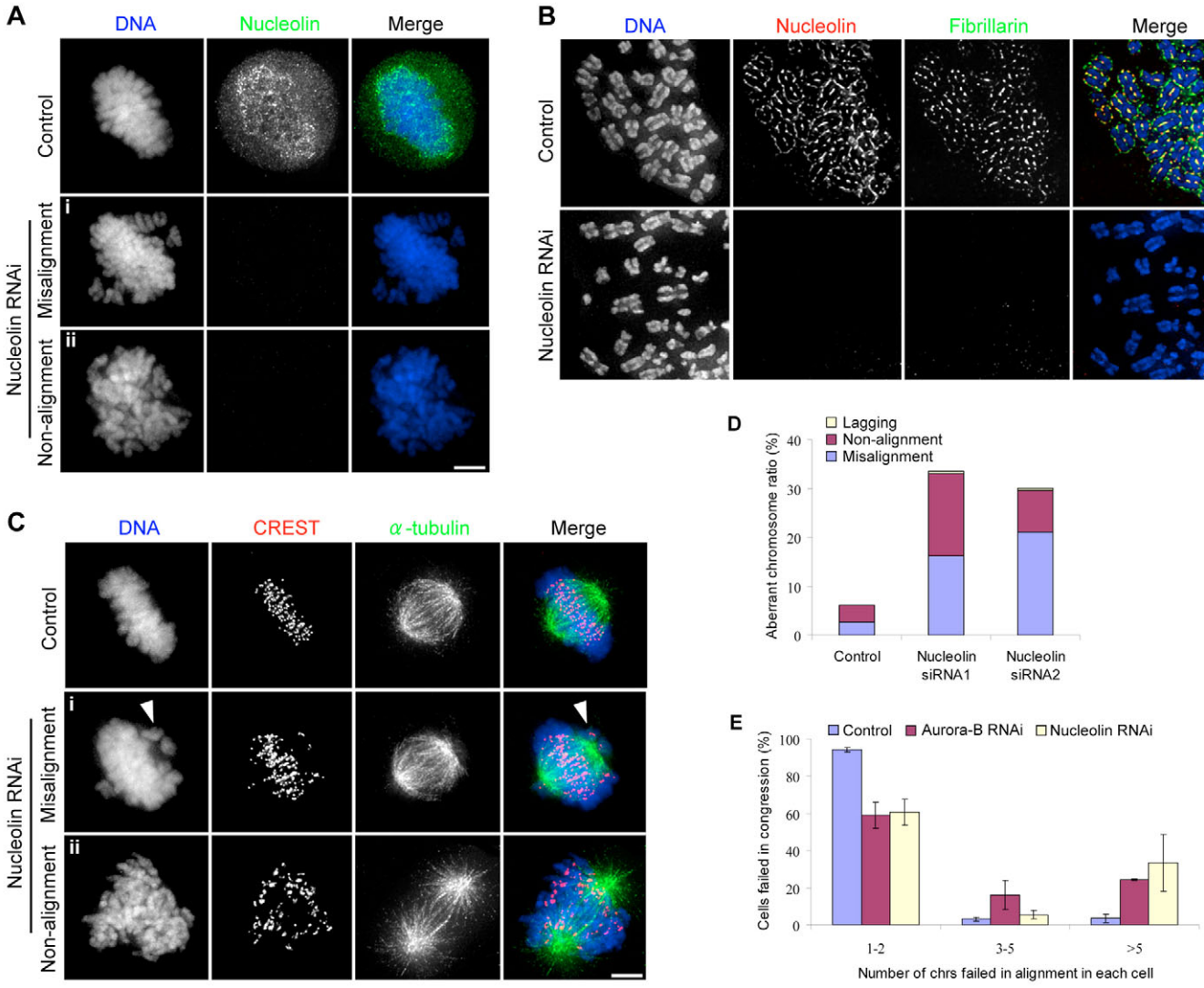

Fig. 4. Nucleolin depletion induces defects in chromosome congression. (A) Mitotic cells stained with an anti-nucleolin antibody. The misalignment (i) and non-alignment (ii) phenotypes are shown. (B) Metaphase chromosome spreads stained with nucleolin (green) and fibrillarin (red) antibodies. (C) Mitotic cells stained with α-tubulin (green) and CREST (red) antibodies. The misalignment (i) and non-alignment (ii) phenotypes are shown. Arrowheads show misaligned chromosomes and the fluorescence signals for CREST at the kinetochores. Bars, 5 μm. (D) Quantification of the distributions of chromosome congression defects following transfections. Values represent the mean of four independent experiments (n=400). (E) Histogram showing the numbers of chromosomes that fail to align in each cell. Values represent the mean of four independent experiments ± s.d. (n=400).

We categorized the defects in chromosome alignment into two groups, designated misaligned chromosomes (one to ten chromosomes were not aligned at the metaphase plate, whereas the majority of the chromosomes were aligned) and non-aligned chromosomes (>10 chromosomes were not aligned at the metaphase plate or chromosomes were scattered throughout the cytoplasm). In the misalignment phenotype, several chromosomes remained near the spindle poles, although the other chromosomes aligned at the spindle equator (Fig. 4Ci). In the non-alignment phenotype, most of the chromosomes remained dispersed (Fig. 4Cii). Mitotic cells depleted by siRNA1 exhibited 16.2±5.5% and 16.9±1.8% of the misalignment and non-alignment phenotypes, respectively (Fig. 4D). Similar to siRNA1, mitotic cells depleted by siRNA2 exhibited 21.1±2.4% and 8.5±1.2% of the misalignment and non-alignment phenotypes, respectively. By contrast, the control cells showed very few populations of each phenotype (2.5±1.5% and 3.4±1.3%, respectively). As a positive control for chromosome congression, we examined the effects of depletion of Aurora-B, a mitotic kinase known to be required for chromosome congression (Hauf et al., 2003). Most of the nucleolin-depleted cells contained only one or a few misaligned chromosomes, and only 33.6% of the cells had five or more misaligned chromosomes (Fig. 4E). These findings demonstrate that human nucleolin is involved in normal chromosome congression.

Nucleolin is involved in correct kinetochore-microtubule attachments

Failure of chromosome congression may be due to an inability of the kinetochore-microtubule interactions to maintain sufficient tension. To verify this hypothesis, the interkinetochore distances, which reflect the accurate tension force (Waters et al., 1996), were measured in kinetochore pairs by staining Aurora-B in the middle of the kinetochores and CENP-A on either side of Aurora-B (Fig. 5A). We found that the average interkinetochore distance decreased from 1.4±0.2 μm in control metaphase cells to 1.1±0.2 μm for non-aligned chromosomes in nucleolin-depleted cells (P<0.001) (Fig. 5B). There was also a 21.4% reduction in centromere stretching relative to the resting length of 1.1±0.1 μm in control prometaphase cells. As a positive control, the interkinetochore distance of cells treated with colcemid was reduced by 34.2% (0.9±0.2 μm) compared with that in control metaphase cells. We also measured the interkinetochore distance of aligned chromosomes in the misalignment phenotype. Unexpectedly, we found an interkinetochore distance of 1.2±0.2 μm, representing reduced sister chromatid stretching compared with that in control metaphase cells (P<0.001).

Nucleolin depletion resulted in a reduction of stretched kinetochores on misaligned or non-aligned sister chromatids, which could indicate that these kinetochores are incorrectly bound to microtubules. When cells were stained with CREST and α-tubulin antibodies, bioriented kinetochore pairs with kinetochore fibers terminating at the kinetochores were frequently observed in control cells (Fig. 5C, enlargement). In the misalignment phenotype, the chromosomes at the spindle equator were attached to microtubules oriented from the opposite spindle poles (Fig. 5D, enlargement a). Although the kinetochores were found to attach to microtubules in nucleolin-depleted cells, the chromosomes often became syntelically attached, i.e. both kinetochores were attached to the same spindle pole (Fig. 5D, enlargement b). Similarly, the dispersed chromosomes also presented syntelic attachments in the non-alignment phenotype (Fig. 5E, enlargements a, b). These defects in biorientation prompted us to analyze the stability of the kinetochore-microtubule attachments. Cells were incubated in ice-cold medium for 10 minutes before fixation to depolymerize all microtubules except stable kinetochore fibers (Rieder, 1981). Control metaphase cells exhibited high levels of tubulin fluorescence. The kinetochore fibers in the nucleolin-depleted cells were considerably diminished (Fig. 5F). In addition, chromosomes located near the spindle poles lacked any associated microtubule staining, indicating that few stable kinetochore-microtubule attachments were present on these chromosomes (Fig. 5F). In conclusion, nucleolin is involved in correct kinetochore-microtubule attachments.

Time-lapse microscopy reveals defective chromosome congression in nucleolin-depleted cells

To define the underlying mechanism responsible for the prometaphase mitotic delay in nucleolin-depleted cells, HeLa cells stably expressing GFP-tagged histone H1.2 (GFP-H1.2) (Gambe et al., 2007) were monitored from prophase. In total, 69.2% of control cells completed mitosis within 1 hour (Fig. 6A,C). Congression was rapid in these control cells and, after nuclear envelope breakdown, all the chromosomes moved quickly towards the spindle equator to achieve full alignment. The situation was quite different in nucleolin-depleted cells. After more than 180 minutes of monitoring, 54.4% of the cells contained various numbers of chromosomes that were unable to migrate to the spindle equator and remained in the vicinity of the spindle poles during congression (Fig. 6B,C). Although nucleolin-depleted cells spent a similar time in prophase to control cells (mean time: 9 minutes), most of the cells showed a very extended prometaphase (mean time: 238 minutes). Nevertheless, metaphase onset was not seen in 42.4% of nucleolin-depleted cells. As time progressed, the chromosomes in these cells gradually became decondensed and then aggregated to form mini-nuclei, a hallmark of cell death. These aberrations were not owing to the experimental conditions, because normal mitotic progression was detected in all the control cells. Only 12% of nucleolin-depleted cells completed cell division with a significant mitotic delay at prometaphase.

To further characterize the defects in chromosome congression after nucleolin depletion, we performed RNAi in HeLa cells stably expressing GFP-tagged CENP-A (GFP-CENP-A) (Kunitoku et al., 2003). In control cells, paired sister kinetochores congressed to the spindle equator and oscillated until anaphase onset (Fig. 6D). In nucleolin-depleted cells, some kinetochore pairs remained at the spindle poles for the duration of the analysis. Frequent oscillation of sister kinetochores was observed, and they moved back and forth between the spindle poles and the spindle equator. These findings indicate that nucleolin plays important roles in both the establishment and maintenance of bioriented kinetochore microtubule attachments.

Nucleolin is involved in spindle assembly

The specificity of the TG-3 antibody, which recognizes nucleolin phosphorylated by CDC2 during mitosis (phospho-nucleolin), was confirmed in a previous study (Dranovsky et

al., 2001). We confirmed its specificity by immunoblotting and immunostaining (Fig. 7A,B). Following transfection of nucleolin siRNAs, quantitative immunoblotting of cell extracts revealed that the phospho-nucleolin level was reduced to 18.7% of the control level. The TG-3 staining pattern in metaphase chromosome spreads was the same as that using an

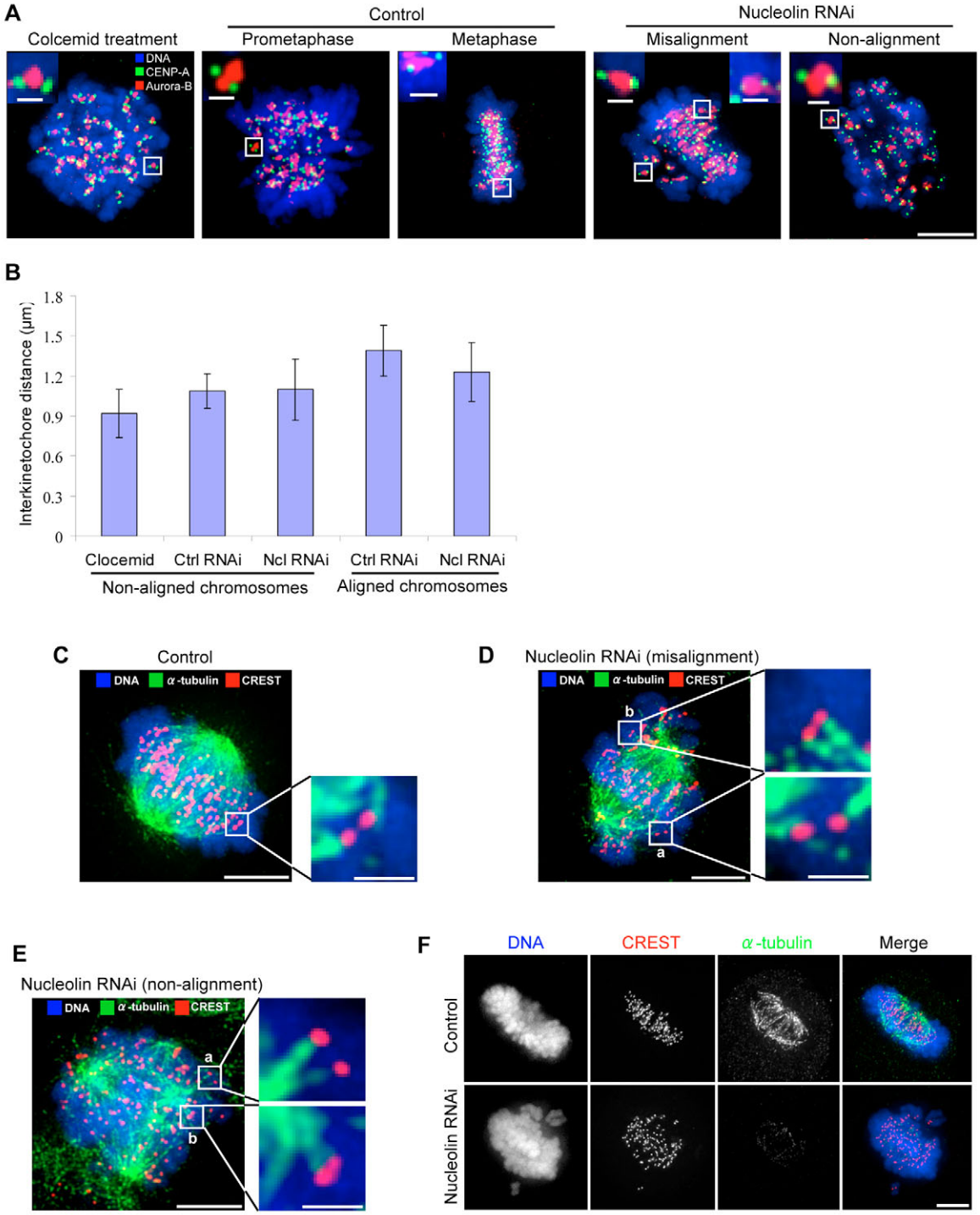

Fig. 5. Nucleolin depletion induces significant reductions in centromere stretching and syntelic kinetochore-microtubule attachments. (A) Analysis of the interkinetochore distances across sister chromatids. Immunostaining for Aurora-B (central) and CENP-A (either side of Aurora-B) is shown in red and green, respectively. Bars, 5 μm; 1.25 μm (enlarged area). (B) Interkinetochore distances of non-aligned and aligned chromosomes following siRNA transfections as indicated. The interkinetochore distances were measured using CENP-A as a marker. Each value was derived by measuring at least 40 kinetochores in more than five cells. Values for non-aligned chromosomes in control cells were obtained at prometaphase. (C) Control metaphase cells stained with CREST (red) and α-tubulin (green) antibodies. (D,E) Misalignment (D) and non-alignment (E) phenotypes stained with CREST (red) and α-tubulin (green) antibodies. (F) Cells were cold-treated and stained with α-tubulin (green) and CREST (red) antibodies.

anti-nucleolin antibody (data not shown). We observed phospho-nucleolin fluorescence at the chromosome periphery and spindle poles in mitotic cells fixed with 4% paraformaldehyde (PFA) (data not shown). The polar localization of phospho-nucleolin was facilitated by detergent treatment before the PFA fixation (data not shown). The association of phospho-nucleolin with the spindle poles was best observed when the cells were fixed with methanol at

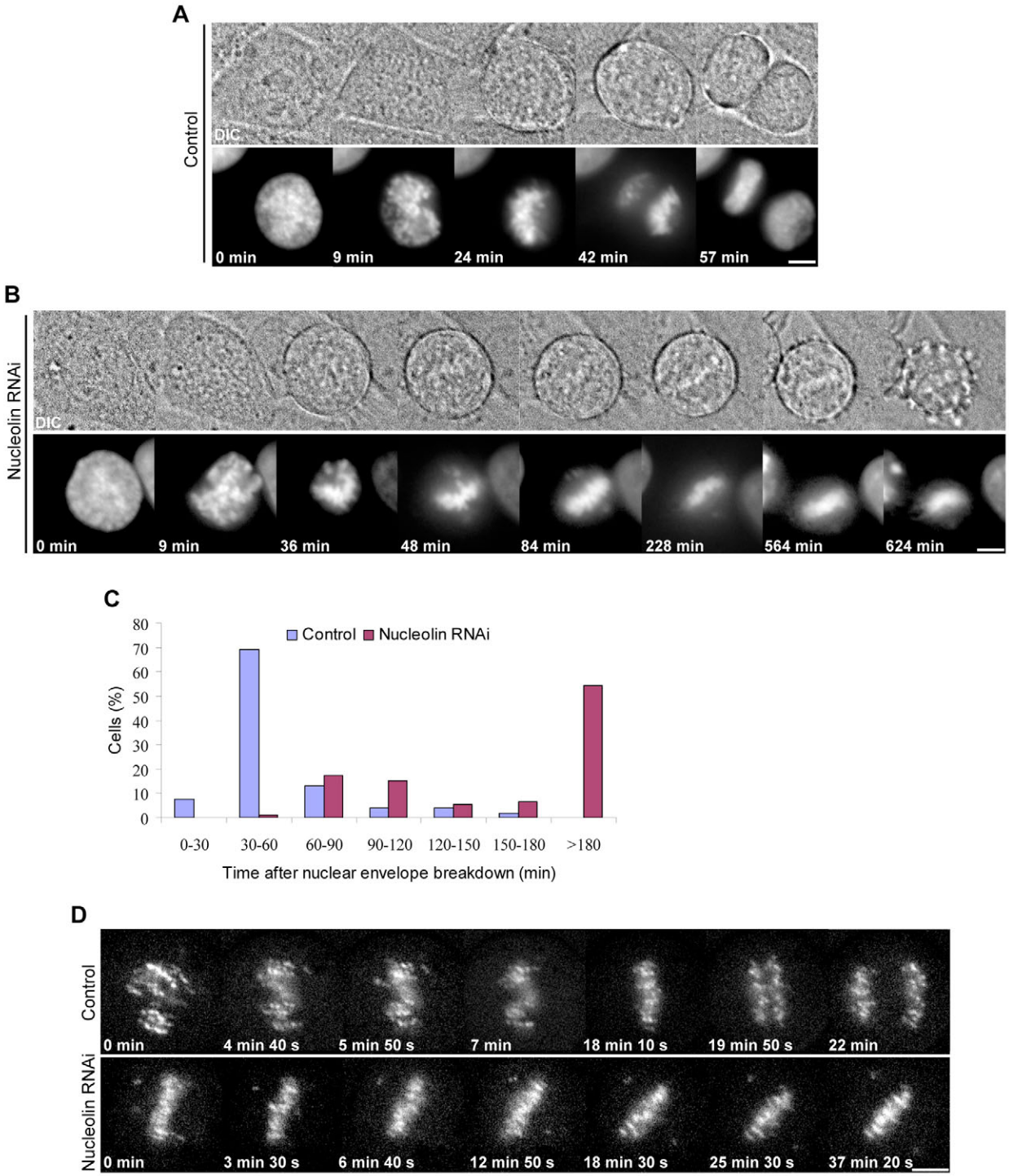

Fig. 6. Nucleolin depletion induces a mitotic block at prometaphase. (A,B) HeLa cells stably expressing histone GFP-H1.2 were imaged by time-lapse fluorescence microscopy after transfection of the indicated siRNAs. Times are given in minutes. DIC, differential interference contrast. (C) Histogram showing the percentages of cells with different durations of mitosis. Fifty-three control cells and 58 nucleolin-depleted cells were analyzed for time-lapse fluorescence microscopy. (D) HeLa cells stably expressing GFP-CENP-A were imaged by time-lapse fluorescence microscopy after transfection of the indicated siRNAs. Times are given in minutes and seconds. Bars, 10 μm.

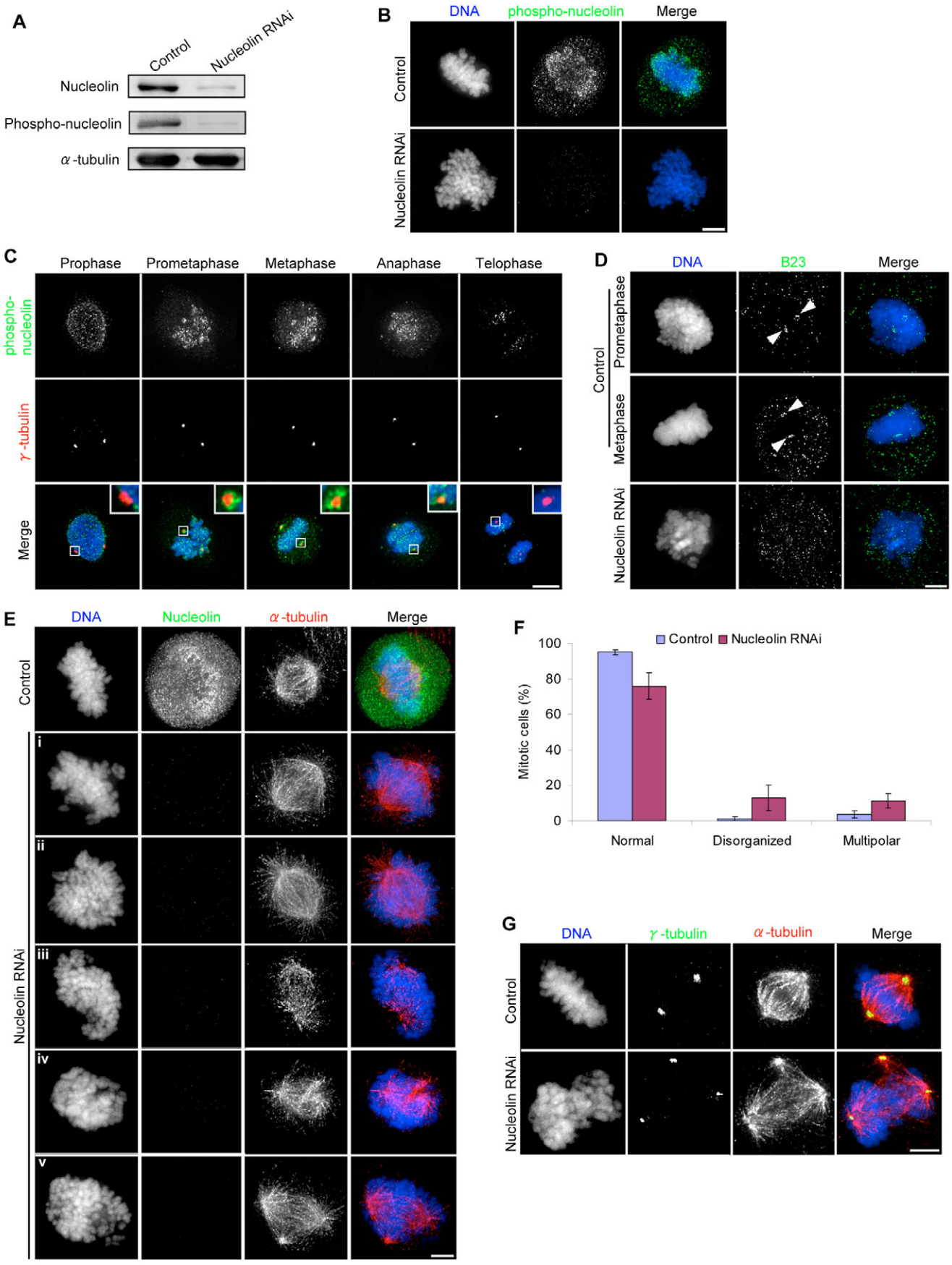

Fig. 7. See next page for legend.

Fig. 7. Nucleolin depletion causes mitotic spindle defects. (A) Immunoblot showing effective depletion of nucleolin and phospho-nucleolin after nucleolin RNAi. α-tubulin is shown as a control. (B) Mitotic cells stained for phosphorylated nucleolin (green). (C) Mitotic cells stained for phosphorylated nucleolin (green) and γ-tubulin (red). (D) Mitotic cells stained for B23 (green). Arrowheads show fluorescence signals for B23 at the spindle poles. (E) Mitotic spindle defects in nucleolin-depleted cells. The majority of cells with chromosome congression defects (i, misalignment; ii, non-alignment) appear to have normal spindles, whereas a small percentage show disorganized (iii and iv) or multipolar (v) spindles. Staining for nucleolin (green) and α-tubulin (red) is shown. (F) Histograms showing quantification of the spindle defects after nucleolin depletion. Values represent the mean of four independent experiments ± s.d. (n=400). (G) Nucleolin depletion induces multiple centrosomes. Staining for γ-tubulin (green) and α-tubulin (red) is shown. Bars, 5 μm.

–20°C (Fig. 7C). With this protocol, labeling of the chromosomes was also observed. Phospho-nucleolin appeared in the vicinity of the spindle poles at prometaphase when the nuclear envelope began to disassemble. It became most prominent at metaphase when the chromosomes became aligned at the spindle equator. At anaphase, when the chromosomes segregated, the staining of the spindle poles became more dispersed. At telophase, phospho-nucleolin appeared within the reforming nuclei and disappeared from the spindle poles. B23, a major phosphoprotein in interphase nucleoli, is associated with the poles of the mitotic spindle and chromosome periphery during mitosis (Zatsepina et al., 1999). Consistent with this previous report, we found that B23 was localized at the spindle poles at prometaphase and metaphase following Triton-X 100 extraction before fixation (Fig. 7D). The polar localization of B23 disappeared after nucleolin depletion (Fig. 7D), although the polar localization of another spindle pole protein, CLASP1, was not affected by the depletion of nucleolin (data not shown).

A multipolar spindle phenotype was defined as the presence of more than two spindle poles within a cell (Fig. 7Ev). The frequencies of disorganized and multipolar spindles were 12.9±7.2% and 11.3±6.4% in nucleolin-depleted mitotic cells, compared with only 1.2±1.3% and 3.8±1.1% in control cells, respectively (Fig. 7F), indicating that the normal function of nucleolin is involved in maintaining the mitotic spindle morphology. When nucleolin-depleted cells were stained for α-tubulin and γ-tubulin, multiple centrosomes were found in the multipolar spindle cells (Fig. 7G), suggesting that nucleolin is involved in regulating centrosome duplication to ensure the formation of a bipolar spindle.

Nucleolin associates with both fibrillarin and B23 during the cell cycle

Since the localizations of both fibrillarin and B23 in the nucleoli or chromosome periphery appeared to be dependent on the presence of nucleolin, it is possible that nucleolin, fibrillarin and B23 are present in a complex in vivo, and that the absence of one of these components could influence the stability of the complex. To investigate this possibility, we immunoprecipitated total cell extracts and synchronized mitotic cell extracts with an anti-nucleolin antibody. We used a double-thymidine block to achieve the mitotic cell synchronization. DNA staining with DAPI demonstrated that, after removal of the thymidine block, about 60% of the cells passed through mitosis over 10 hours (data not shown). Consistent with previous reports (Yanagida et al., 2001; Yanagida et al., 2004), physical associations of nucleolin with fibrillarin (Fig. 8A) and B23 (data not shown) were detected in the total cell extracts. Fibrillarin and B23 remained associated with nucleolin in complexes in the synchronized mitotic cells (Fig. 8B).

Discussion

Nucleolin is required for nucleolus formation

When nucleolin was depleted, dispersed nucleoli were observed. Simultaneously, nucleolar proteins including fibrillarin, B23 and Ki-67 showed no systematic localizations in the nucleoli. Similar to nucleolin, fibrillarin and B23 have been identified in ribonucleoprotein complexes (Yanagida et al., 2001), although the relationship between Ki-67 and nucleolin remains unclear. Since Ki-67 is also dispersed in nucleoli after nucleolin depletion, we hypothesize that the apparent nucleolar dispersions of these three proteins in nucleolin-depleted cells probably arise as a consequence of disorganization of the nucleolar structure. It has been reported that mutations in genes encoding nucleolin homologues in fission yeast (*GAR2*) and *Arabidopsis* (*AtNUC-L1*) have severe effects on the organization of nucleoli (Léger-Silvestre et al., 1997; Pontvianne et al., 2007). However, the function of nucleolin in the organization of nucleoli has not been reported in animal cells. The present study is the first description of an essential role for human nucleolin in maintaining the nucleolar structure.

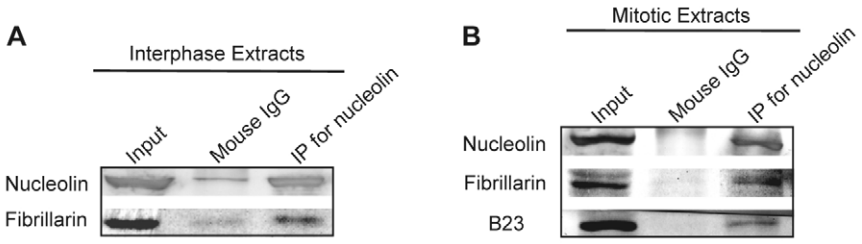

Fig. 8. Immunoblot analysis of nucleolin-binding complexes from total cell extracts and synchronized mitotic cell extracts. Nucleolin-binding complexes were pulled down from total cell extracts (A) and synchronized mitotic cell extracts (B) by an anti-nucleolin antibody. To obtain the synchronized mitotic cell extracts, cells under double-thymidine block were released for approximately 10 hours, and then lysed for immunoblotting detection. Protein G beads coupled with mouse IgG were used as a control.

Nucleoli were recently shown to be dynamic subnuclear bodies, because the residence times of most nucleolar proteins are in the order of tens of seconds (Phair and Misteli, 2000; Chen and Huang, 2001). In reality, the structure of a nucleolus is the total sum of the molecules entering and leaving a given subnuclear space, with the residence times of individual molecules governing its overall organization (Olson and Dundr, 2005). These residence times are determined by interactions between nucleolar molecules. Thus, when the amount of nucleolar nucleolin is reduced by RNAi, fibrillarin, B23 and Ki-67 could lose their affinities for other nucleolar components, which finally results in their shorter residence times in the nucleolus. Fibrillarin is involved in all the major post-transcriptional activities in ribosome synthesis, the first steps of rRNA processing, pre-rRNA modification and ribosome assembly (Tollervey et al., 1993). Similar to nucleolin depletion, microinjection of anti-fibrillarin antibodies can also induce defects in nucleolus formation (Fomproix et al., 1998).

In conclusion, all these data suggest that nucleolar proteins, including nucleolin and fibrillarin, which are involved in ribosome biogenesis, play important roles in nucleolus formation. Consistent with an earlier hypothesis that a subset of ribonucleoprotein complexes remains assembled and becomes incorporated into the new nucleolus (Medina et al., 1995; Piñol-Roma et al., 1999), associations of nucleolin with fibrillarin and B23 were found during the cell cycle. It seems likely that these interactions between nucleolin and nucleolar proteins, including fibrillarin and B23, are of physical significance, because we have demonstrated that nucleolin is required in order to retain fibrillarin and B23 in the nucleoli and chromosome periphery.

Nucleolin is involved in chromosome congression

In nucleolin-depleted HeLa cells, chromosome congression to the spindle equator was delayed. This could be due to activation of the spindle checkpoint in response to improper kinetochore-microtubule attachments, such as those demonstrated for chromosomes stuck at the spindle poles during prometaphase. Recent data have shown that Aurora-B plays an important role in correction of improper microtubule-kinetochore interactions, such as syntelic or merotelic attachments (Hauf et al., 2003; Cimini et al., 2006). Activation of Aurora-B during mitosis can correct chromosome attachment errors by selective disassembly of kinetochore-microtubule fibers, thereby activating the spindle checkpoint until all the chromosomes make proper bipolar attachments to the mitotic spindle. It is therefore probable that nucleolin depletion does not activate the checkpoint directly but rather causes an increase in syntelic attachments, which are changed into unattached kinetochores by Aurora-B.

Electron microscopy studies have revealed that the plus ends of spindle microtubules terminate in the outer kinetochore of vertebrate cells (McEwen et al., 1998; VandenBeldt et al., 2006), suggesting that nucleolin covering the outermost layer of kinetochores could affect the kinetochore-microtubule attachments. We found that cells depleted of nucleolin were delayed at prometaphase with misaligned or non-aligned chromosomes and defects in chromosome biorientation. Aligned chromosomes exhibited reduced centromere stretching and diminished kinetochore-microtubule fibers. Our data suggest that nucleolin is involved in efficient kinetochore-microtubule interactions and/or the stabilization of such interactions. These interactions must be correct to allow normal chromosome congression and segregation. We did observe syntelic attachments in the misaligned or non-aligned chromosomes of nucleolin-depleted cells (Fig. 5D,E), and these may hinder the formation of proper attachments. Our evidence reveals that nucleolin is not required for kinetochore assembly. Specifically, the evidence for this conclusion includes the following: (1) nucleolin depletion does not affect the localizations of kinetochore proteins, including Aurora-B (data not shown), Bub1 (Fig. 3D), BubR1 (Fig. 3E), CENP-A (Fig. 5A), CENP-E (data not shown), Hec1 (data not shown) and Mad2 (Fig. 3F); and (2) kinetochores can capture microtubules in the absence of nucleolin (Fig. 5D,E).

One possibility is that disruption of the nucleoli per se perturbes chromosome congression, mitotic progression and/or spindle formation. However, depletion of certain nucleolar proteins, such as UBF (Rubbi and Milner, 2003) and TIF-IA (Yuan et al., 2005) localized in the nucleolus organizer region during mitosis (Roussel et al., 1993; Prieto and McStay, 2005), by antibody microinjection or genetic inactivation did not lead to mitotic delay or defects in chromosome congression, although disorganized nucleoli were observed. Therefore, our reported mitotic abnormalities are not caused by nucleolar disorganization but rather depletion of nucleolin. To the best of our knowledge, this is the first report that a chromosome peripheral protein can contribute to chromosome congression during mitosis.

Nucleolin is involved in the maintenance of mitotic spindle integrity

Movement of a chromosome on the mitotic spindle is mediated by the formation of a bundle of microtubules that tethers the kinetochore on the chromosome to a spindle pole. Mechanical linkages between chromatids and microtubules are crucially important for spindle assembly (Cassimeris and Skibbens, 2003). Since nucleolin is important for the stability of kinetochore-microtubule attachments, we suspect that the mitotic spindle disorganization observed in nucleolin-depleted cells is the consequence of a defect in the kinetochore-microtubule attachments. Consistent with this hypothesis, abrogation of kinetochore-microtubule attachments by depleting certain kinetochore proteins, including CENP-F (Holt et al., 2005), hMis12 (Goshima et al., 2003), NDC80 complex (Bharadwaj et al., 2004), CENP-A (Regnier et al., 2005) and Shugoshin (Salic et al., 2004), can lead to overt spindle defects.

Protein phosphorylation has been proposed as an important control mechanism for the events leading to the initiation and completion of mitosis (Vandre et al., 1984). Numerous phosphoproteins relocate to the spindle poles during mitosis (Vandre et al., 1984; Vandré and Burry, 1992). Meanwhile, nucleolin is highly phosphorylated by CDC2 during mitosis (Belenguer et al., 1990; Peter et al., 1990). Here, we report for the first time that nucleolin is also present in the vicinity of the spindle poles during mitosis. Using standard PFA cell fixation, we were able to observe both nucleolin localizations, and found that the stronger signal emerged from the chromosome periphery, whereas the weaker one arose from the spindle poles. In the vast majority of mitotic cells fixed with aldehydes,

it was obvious that the polar nucleolin labeling was masked by the cytoplasmic mass. This may explain why the presence of nucleolin at the spindle poles has not yet been described. Therefore, application of a fixation procedure that is known to preserve the cytoskeleton makes it possible to detect the nucleolin signals in the spindle poles.

In the present study, we found that the frequencies of cells with multipolar spindles were much higher among nucleolin-depleted cells than among control cells, and this phenomenon is probably caused by the existence of supernumerary centrosomes. It has been reported that B23 is involved in regulating centrosome duplication in the cell cycle (Okuda, 2002; Wang et al., 2005). Since nucleolin depletion resulted in a dramatic reduction in the spindle pole localization of B23, it is possible that nucleolin also plays a role in centrosome duplication through its interaction with B23, which is also known to be phosphorylated by CDC2 kinase at the onset of mitosis (Peter et al., 1990). Furthermore, hyperphosphorylated B23 isoforms are specifically associated with the spindle poles (Zatsepina et al., 1999). Here, we report similar behavior for nucleolin, since its phosphorylated isoform was associated with the spindle poles. Furthermore, the nucleolin in the vicinity of the spindle poles resisted extraction with detergent before fixation, whereas that in the chromosome periphery largely disappeared under the same conditions (data not shown), suggesting that the properties of these two types of nucleolin are different. Therefore, mapping and mutation of the nucleolin in the vicinity of the spindle poles will be necessary to investigate the functions of this particular, yet previously undescribed, nucleolin isoform.

Materials and Methods

Cell line

HeLa cells were grown in Dulbecco's modified Eagle's medium (DMEM; GIBCO BRL) supplemented with 10% fetal bovine serum (Equitech-Bio Inc.) and penicillin.

Cell synchronization by colcemid treatment and double-thymidine block

Mitotic arrest was induced by adding 100 ng/ml colcemid to the culture medium and incubating the cells for 16 hours. For mitosis synchronization, cells were treated twice with 2.5 mM thymidine (Sigma) for 16 hours each, separated by a 10-hour exposure to culture medium, and then released from the block by incubation with culture medium. After approximately 10 hours, approximately 60% of the cells passed through mitosis.

Depletion of nucleolin and Aurora-B in HeLa cells by RNAi

A nonspecific siRNA duplex (Qiagen) was used for control transfections. Two siRNA duplexes (siRNA1: 5′-AGAGUUUGCUUCAUUCGAATT-3′; and siRNA2: 5′-GACAGUGAUGAAGAGGAGGTT-3′) targeting human nucleolin were used to deplete nucleolin. Previously reported siRNA duplexes for Aurora-B (Ditchfield et al., 2003) were used to deplete Aurora-B. HeLa cells were transfected with siRNA duplexes using Lipofectamine 2000 (Invitrogen), and then subjected to immunoblotting and immunostaining analyses at 72 hours after the transfections.

Antibodies

The antibodies against the following proteins were used as follows: nucleolin (mouse monoclonal; 1:100 dilution; Santa Cruz Biotechnology); Ki-67 (mouse monoclonal; 1:200 dilution; DakoCytomation); α-tubulin (mouse monoclonal; 1:200 dilution; Calbiochem); α-tubulin (rabbit polyclonal; 1:200 dilution; Abcam); γ-tubulin (rabbit monoclonal; 1:1000 dilution; Sigma); BubR1 (mouse monoclonal; 1:500 dilution; BD Transduction Laboratories); Bub1 (mouse monoclonal; 1:50 dilution; Chemicon); CENP-E (mouse monoclonal; 1:100 dilution; Abcam); CENP-A (mouse monoclonal; 1:50 dilution; Abcam); Aurora-B (rabbit polyclonal, 1:1000 dilution; Abcam); fibrillarin (rabbit polyclonal; 1:100 dilution; Abcam); anti-centromere autoimmune serum (CREST; (human monoclonal; 1:100 dilution; Cortex Biochem); Hec1 (mouse monoclonal; 1:100 dilution; ABR-Affinity BioReagents); Mad2 (rabbit polyclonal; 1:100 dilution; Covance), B23 (goat polyclonal; 1:50 dilution; Santa Cruz Biotechnology), hnRNP-U (mouse monoclonal; 1:250 dilution; Abcam); CDC27 (mouse monoclonal; 1:250 dilution; Abcam); CDC20 (mouse monoclonal; 1:250 dilution; MBL); cyclin B1 (rabbit monoclonal; 1:250 dilution; Sigma); and β-actin (mouse monoclonal; 1:500 dilution; Sigma). The TG-3 antibody against phosphorylated nucleolin was obtained from Peter Davies (Albert Einstein College of Medicine in Yeshiva University, New York). The anti-CLASP1 antibody was obtained from William Earnshaw (Wellcome Trust Centre for Cell Biology, University of Edinburgh).

Microscopy and image analyses

All cell preparations were examined using a deconvolution microscopy system (DeltaVision; Applied Precision) and oil immersion objectives. The fluorescence intensities of the signals were analyzed with the Image J program (http://rsb.info.nih.gov/ij/download.html). The interkinetochore distances were measured as previously described (Waters et al., 1996). The distances were determined in at least five cells (40 kinetochore pairs).

For living cell imaging, the medium was replaced with a CO_2-independent medium supplemented with 10% fetal bovine serum, penicillin-streptomycin and L-glutamine (Invitrogen), and covered with mineral oil immediately before analysis. Cells were maintained at 37°C using a heated stage. Images of cells expressing GFP-H1.2 were collected under an inverted microscope (Olympus IX81) using a 40×NA 1.4 planApo objective. The acquisition parameters, including exposure, focus and illumination, were controlled by the MetaMorph software (Universal Imaging). Single focal plane images were collected by a camera at 3-minute intervals. To capture images of cells expressing GFP-CENP-A, three *z*-sections were acquired at 1-μm steps at 10-second time intervals. The *z*-stacks were projected using the MetaMorph software. All subsequent analyses and processing of images were performed using the MetaMorph software.

Immunostaining of HeLa cells and metaphase chromosome spreads

HeLa cells on poly-L-lysine-coated coverslips were fixed in 4% PFA in PBS for 10 minutes at 37°C and then permeabilized in 0.2% Triton X-100 in PBS for 10 minutes. Next, the cells were blocked with 1% BSA in PBS for 30 minutes, and sequentially incubated with primary and secondary antibodies diluted in 1% BSA in PBS for 1 hour. All the incubation steps were carried out at 37°C. For some antibodies (CENP-E and γ-tubulin), immunostaining analyses were carried out as previously described (Forgues et al., 2003). For staining of Bub1 and phosphorylated nucleolin, cells were fixed in methanol for 10 minutes at –20°C. Immunostaining for B23 was performed as previously described (Zatsepina et al., 1999). Immunostaining of metaphase chromosome spreads was performed as previously described (Ono et al., 2003), except that the cells were treated with 75 mM KCl at room temperature for 15 minutes rather than at 37°C for 30 minutes.

Immunoblotting

Following extraction of transfected cells with SDS sample buffer, the protein extracts were separated by SDS-PAGE and transferred to PVDF membranes for immunoblotting. The immunoblots were blocked with 0.1% BSA in TBST (0.1% Tween 20, 25 mM Tris-HCl pH 7.4, 137 mM NaCl, 25 mM KCl) and then sequentially incubated with primary and secondary antibodies diluted in TBST. Finally, the immunoreactive protein bands were detected by NBT/BCIP solution (Roche) supplemented with AP buffer (100 mM Tris-HCl pH 9.5, 100 mM NaCl, 1 mM $MgCl_2$).

Immunoprecipitation

Immunoprecipitation was carried out using a mouse monoclonal antibody against nucleolin, or normal mouse IgG (Santa Cruz Biotechnology) as a control. The antibodies were bound to protein G-Sepharose (GE Healthcare) containing 0.1% BSA, 150 mM NaCl, 20 mM Tris-HCl pH 8.0 and 0.05% Tween 20 by rocking at 4°C overnight. HeLa cells were harvested by centrifugation at 310 ***g*** for 5 minutes, rinsed with PBS and centrifuged again at 310 ***g***. Cell pellets were stored at –80°C until analysis. The cells were extracted in 5 volumes of buffer A [10% cell lysis buffer (Cell Signaling), 0.1% SDS, protease inhibitor cocktail (Roche)] for 30 minutes, and centrifuged at 15,100 ***g*** for 30 minutes. To reduce the amount of proteins nonspecifically binding to the beads, the supernatant was first rocked with beads for 30 minutes at 4°C. After centrifugation, the supernatant was incubated with antibody-bead complexes for 3 hours at 4°C. Next, the beads were collected by centrifugation and washed five times in buffer A. Finally, protein-bead complexes were solubilized by boiling, centrifuged, subjected to SDS-PAGE and analyzed by immunoblotting.

This work was supported by Grants-in-Aid for Scientific Research from the Ministry of Education, Science, Culture, Sports, Science and Technology of Japan to K.F., S.M. and S.U. and by an Industrial Technology Research Grant Program in 2003 from the New Energy and Industrial Technology Development Organization (NEDO) of Japan to S.M. We thank Peter Davies for the anti-phospho-nucleolin antibody, William C. Earnshaw for the anti-CLASP1 antibody and Toru Hirota for the HeLa cells stably expressing GFP-CENP-A.

References

Angelov, D., Bondarenko, V. A., Almagro, S., Menoni, H., Mongelard, F., Hans, F., Mietton, F., Studitsky, V. M., Hamiche, A., Dimitrov, S. et al. (2006). Nucleolin is a histone chaperone with FACT-like activity and assists remodeling of nucleosomes. *EMBO J.* **25**, 1669-1679.

Azum-Gélade, M. C., Noaillac-Depeyre, J., Caizergues-Ferrer, M. and Gas, N. (1994). Cell cycle redistribution of U3 snRNA and fibrillarin. Presence in the cytoplasmic nucleolus remnant and in the prenucleolar bodies at telophase. *J. Cell Sci.* **107**, 463-475.

Becherel, O. J., Gueven, N., Birrell, G. W., Schreiber, V., Suraweera, A., Jakob, B., Taucher-Scholz, G. and Lavin, M. F. (2006). Nucleolar localization of aprataxin is dependent on interaction with nucleolin and on active ribosomal DNA transcription. *Hum. Mol. Genet.* **15**, 2239-2249.

Belenguer, P., Caizergues-Ferrer, M., Labbe, J. C., Dorée, M. and Amalric, F. (1990). Mitosis-specific phosphorylation of nucleolin by $p34^{cdc2}$ protein kinase. *Mol. Cell. Biol.* **10**, 3607-3618.

Bertuch, A. A. and Lundblad, V. (2003). The Ku heterodimer performs separable activities at double-strand breaks and chromosome termini. *Mol. Cell. Biol.* **23**, 8202-8215.

Bharadwaj, R., Qi, W. and Yu, H. (2004). Identification of two novel components of the human NDC80 kinetochore complex. *J. Biol. Chem.* **279**, 13076-13085.

Biqqioqera, M., Burki, K., Kaufmann, S. H., Shaper, J. H., Gas, N., Amalric, F. and Fakan, S. (1990). Nucleolar distribution of proteins B23 and nucleolin in mouse preimplantation embryos as visualized by immunoelectron microscopy. *Development* **110**, 1263-1270.

Caizergues-Ferrer, M., Mariottini, P., Curie, C., Lapeyre, B., Gas, N., Amalric, F. and Amaldi, F. (1989). Nucleolin from *Xenopus Laevis*: cDNA cloning and expression during development. *Genes Dev.* **3**, 324-333.

Cassimeris, L. and Skibbens, R. V. (2003). Regulated assembly of the mitotic spindle: a perspective from two ends. *Curr. Issues Mol. Biol.* **5**, 99-112.

Chen, D. and Huang, S. (2001). Nucleolar components involved in ribosome biogenesis cycle between the nucleolus and nucleoplasm in interphase cells. *J. Cell Biol.* **153**, 169-176.

Cimini, D., Wan, X., Hirel, C. B. and Salmon, E. D. (2006). Aurora kinase promotes turnover of kinetochore microtubules to reduce chromosome segregation errors. *Curr. Biol.* **16**, 1711-1718.

Didier, D. K. and Klee, H. J. (1992). Identification of an Arabidopsis DNA-binding protein with homology to nucleolin. *Plant Mol. Biol.* **18**, 977-979.

Ditchfield, C., Johnson, V. L., Tighe, A., Ellston, R., Haworth, C., Johnson, T., Mortlock, A., Keen, N. and Taylor, S. S. (2003). Aurora B couples chromosome alignment with anaphase by targeting BubR1, Mad2, and Cenp-E to kinetochores. *J. Cell Biol.* **161**, 267-280.

Dranovsky, A., Vincent, I., Gregori, L., Schwarzman, A., Colflesh, D., Enghild, J., Strittmatter, W., Davies, P. and Goldgaber, D. (2001). Cdc2 phosphorylation of nucleolin demarcates mitotic stages and Alzheimer's disease pathology. *Neurobiol. Aging* **22**, 517-528.

Dundr, M., Meier, U. T., Lewis, N., Rekosh, D., Hammarskjöld, M. L. and Olson, M. O. J. (1997). A class of nonribosomal nucleolar components is located in chromosome periphery and in nucleolus-derived foci during anaphase and telophase. *Chromosoma* **105**, 407-417.

Fomproix, N., Gebrane-Younes, J. and Hernandez-Verdun, D. (1998). Effects of anti-fibrillarin antibodies on building of functional nucleoli at the end of mitosis. *J. Cell Sci.* **111**, 359-372.

Forgues, M., Difilippantonio, M. J., Linke, S. P., Ried, T., Nagashima, K., Feden, J., Valerie, K., Fukasawa, K. and Wang, X. W. (2003). Involvement of Crm1 in hepatitis B virus X protein-induced aberrant centriole replication and abnormal mitotic spindles. *Mol. Cell. Biol.* **23**, 5282-5292.

Gambe, A. G., Maniwa, R., Matsunaga, S., Kutsuna, N., Higaki, T., Higashi, T., Hasezawa, S., Uchiyama, S. and Fukui, K. (2007). Development of a multistage classifier for a monitoring system of cell activity based on imaging of chromosomal dynamics. *Cytometry A* **71**, 286-296.

Gautier, T., Dauphin-Villemant, C., André, C., Masson, C., Arnoult, J. and Hernandez-Verdun, D. (1992a). Identification and characterization of a new set of nucleolar ribonucleoproteins which line the chromosomes during mitosis. *Exp. Cell Res.* **200**, 5-15.

Gautier, T., Masson, C., Quintana, C., Arnoult, J. and Hernandez-Verdun, D. (1992b). The ultrastructure of the chromosome periphery in human cell lines. An in situ study using cryomethods in electron microscopy. *Chromosoma* **101**, 502-510.

Ginisty, H., Sicard, H., Roger, B. and Bouvet, P. (1999). Structure and functions of nucleolin. *J. Cell Sci.* **112**, 761-772.

Goshima, G., Kiyomitsu, T., Yoda, K. and Yanagida, M. (2003). Human centromere chromatin protein hMis12, essential for equal segregation, is independent of CENP-A loading pathway. *J. Cell Biol.* **160**, 25-39.

Gotzmann, J., Eger, A., Meissner, M., Grimm, R., Gerner, C., Sauermann, G. and Foisner, R. (1997). Two-dimensional electrophoresis reveals a nuclear matrix-associated nucleolin complex of basic isoelectric point. *Electrophoresis* **18**, 2645-2653.

Gulli, M. P., Girard, J. P., Zabetakis, D., Lapeyre, B., Melese, T. and Caizergues-Ferrer, M. (1995). gar2 is a nucleolar protein from *Schizosaccharomyces pombe* required for 18S rRNA and 40S ribosomal subunit accumulation. *Nucleic Acids Res.* **23**, 1912-1918.

Hauf, S., Cole, R. W., LaTerra, S., Zimmer, C., Schnapp, G., Walter, R., Heckel, A., van Meel, J., Rieder, C. L. and Peters, J. M. (2003). The small molecule Hesperadin reveals a role for Aurora B in correcting kinetochore-microtubule attachment and in maintaining the spindle assembly checkpoint. *J. Cell Biol.* **161**, 281-294.

Hernandez-Verdun, D. (2005). Nucleolus: from structure to dynamics. *Histochem. Cell Biol.* **125**, 127-137.

Hernandez-Verdun, D. and Gautier, T. (1994). The chromosome periphery during mitosis. *BioEssays* **16**, 179-185.

Holt, S. V., Vergnolle, M. A. S., Hussein, D., Wozniak, M. J., Allan, V. J. and Taylor, S. S. (2005). Silencing Cenp-F weakens centromeric cohesion, prevents chromosome alignment and activates the spindle checkpoint. *J. Cell Sci.* **118**, 4889-4900.

Kametaka, A., Takagi, M., Hayakawa, T., Haraguchi, T., Hiraoka, Y. and Yoneda, Y. (2002). Interaction of the chromatin compaction-inducing domain (LR domain) of Ki-67 antigen with HP1 proteins. *Genes Cells* **7**, 1231-1242.

Khurts, S., Masutomi, K., Delgermaa, L., Arai, K., Oishi, N., Mizuno, H., Hayashi, N., Hahn, W. C. and Murakami, S. (2004). Nucleolin interacts with telomerase. *J. Biol. Chem.* **279**, 51508-51515.

Kill, I. R. (1996). Localisation of the Ki-67 antigen within the nucleolus. Evidence for a fibrillarin-deficient region of the dense fibrillar component. *J. Cell Sci.* **109**, 1253-1263.

Kunitoku, N., Sasayama, T., Marumoto, T., Zhang, D., Honda, S., Kobayashi, O., Hatakeyama, K., Ushio, Y., Saya, H. and Hirota, T. (2003). CENP-A phosphorylation by Aurora-A in prophase is required for enrichment of Aurora-B at inner centromeres and for kinetochore function. *Dev. Cell* **5**, 853-564.

Léger-Silvestre, I., Gulli, M. P., Noaillac-Depeyre, J., Faubladier, M., Sicard, H., Caizergues-Ferrer, M. and Gas, N. (1997). Ultrastructural changes in the *Schizosaccharomyces pombe* nucleolus following the disruption of the gar2+ gene, which encodes a nucleolar protein structurally related to nucleolin. *Chromosoma* **105**, 542-552.

McEwen, B. F., Hsieh, C. E., Mattheyses, A. L. and Rieder, C. L. (1998). A new look at kinetochore structure in vertebrate somatic cells using high-presure freezing and freeze substitution. *Chromosoma* **107**, 366-375.

Medina, F. J., Cerdido, A. and Fernández-Gómez, M. E. (1995). Components of the nucleolar processing complex (pre-rRNA, fibrillarin, and nucleolin) colocalize during mitosis and are incorporated to daughter cell nucleoli. *Exp. Cell Res.* **221**, 111-125.

Mi, Y., Thomas, S. D., Xu, X., Casson, L. K., Miller, D. M. and Bates, P. J. (2003). Apoptosis in leukemia cells is accompanied by alterations in the levels and localization of nucleolin. *J. Biol. Chem.* **278**, 8572-8579.

Morimoto, H., Ozaki, A., Okamura, H., Yoshida, K., Amorim, B. R., Tanaka, H., Kitamura, S. and Haneji, T. (2005). Differential expression of protein phosphatase type 1 isotypes and nucleolin during cell cycle arrest. *Cell Biochem. Funct.* Doi: 10.1002/cbf.1300.

Okuda, M. (2002). The role of nucleophosmin in centrosome duplication. *Oncogene* **21**, 6170-6174.

Olson, M. O. J. and Dundr, M. (2005). The moving parts of the nucleolus. *Histochem. Cell Biol.* **123**, 203-216.

Olson, M. O., Ezrailson, E. G., Guetzow, K. and Busch, H. (1975). Localization and phosphorylation of nuclear, nucleolar and extranucleolar non-histone proteins of Novikoff hepatoma ascites cells. *J. Mol. Biol.* **97**, 611-619.

Ono, T., Losada, A., Hirano, M., Myers, M. P., Neuwald, A. F. and Hirano, T. (2003). Differential contributions of condensin I and condensin II to mitotic chromosome architecture in vertebrate cells. *Cell* **115**, 109-121.

Peter, M, Nakagawa, J., Dorée, M., Labbé, J. C. and Nigg, E. A. (1990). Identification of major nucleolar proteins as candidate mitotic substrates of cdc2 kinase. *Cell* **60**, 791-801.

Phair, R. D. and Misteli, T. (2000). High mobility of proteins in the mammalian cell nucleus. *Nature* **404**, 604-605.

Piñol-Roma, S. (1999). Association of nonribosomal nucleolar proteins in ribonucleoprotein complexes during interphase and mitosis. *Mol. Biol. Cell* **10**, 77-90.

Pontvianne, F., Matía, I., Douet, J., Tourmente, S., Medina, F. J., Echeverria, M. and Sáez-Vásquez, J. (2007). Characterization of AtNUC-L1 reveals a central role of nucleolin in nucleolus organization and silencing of AtNUC-L2 gene in *Arabidopsis*. *Mol. Biol. Cell* **18**, 369-379.

Prieto, J. L. and McStay, B. (2005). Nucleolar biogenesis: the first small steps. *Biochem. Soc. Trans.* **33**, 1441-1443.

Rao, S. V., Mamrack, M. D. and Olson, M. O. (1982). Localization of phosphorylated highly acidic regions in the NH2-terminal half of nucleolar protein C23. *J. Biol. Chem.* **257**, 15035-15041.

Regnier, V., Vagnarelli, P., Fukagawa, T., Zerjal, T., Burns, E., Trouche, D., Earnshaw, W. and Brown, W. (2005). CENP-A is required for accurate chromosome segregation and sustained kinetochore association of BubR1. *Mol. Cell. Biol.* **25**, 3967-3981.

Rieder, C. L. (1981). The structure of the cold-stable kinetochore fiber in metaphase PtK_1 cells. *Chromosoma* **84**, 145-158.

Roussel, P., Andre, C., Masson, C., Geraud, G. and Hernandez-Verdun, D. (1993). Localization of the RNA polymerase I transcription factor hUBF during the cell cycle. *J. Cell Sci.* **104**, 327-337.

Rubbi, C. P. and Milner, J. (2003). Disruption of the nucleolus mediates stabilization of p53 in response to DNA damage and other stresses. *EMBO J.* **22**, 6068-6077.

Saiwaki, T., Kotera, I., Sasaki, M., Takagi, M. and Yoneda, Y. (2005). In vivo dynamics and kinetics of pKi-67: transition from a mobile to an immobile form at the onset of anaphase. *Exp. Cell Res.* **308**, 123-134.

Salic, A., Waters, J. C. and Mitchison, T. J. (2004). Vertebrate shugoshin links sister centromere cohesion and kinetochore microtubule stability in mitosis. *Cell* **118**, 567-578.

Scholzen, T., Endl, E., Wohlenberg, C., van der Sar, S., Cowell, I. G., Gerdes, J. and Singh, P. B. (2002). The Ki-67 protein interacts with members of the heterochromatin

protein 1 (HP1) family: a potential role in the regulation of higher-order chromatin structure. *J. Pathol.* **196**, 135-144.
Sharp, L. W. (1929). Structure of large somatic chromosomes. *Bot. Gaz.* **88**, 349-382.
Shaw, P. and Doonan, J. (2005). The nucleolus. Playing by different rules? *Cell Cycle* **4**, 102-105.
Srivastava, M. and Pollard, H. B. (1999). Molecular dissection of nucleolin's role in growth and cell proliferation: new insights. *FASEB J.* **13**, 1911-1922.
Suzuki, N., Saito, T. and Hosoya, T. (1987). *In vivo* effects of dexamethasone and cycloheximide on the phosphorylation of 110-kDa proteins and protein kinase activities of rat liver nucleoli. *J. Biol. Chem.* **262**, 4696-4700.
Takagi, M., Matsuoka, Y., Kurihara, T. and Yoneda, Y. (1999). Chmadrin: a novel Ki-67 antigen-related perichromosomal protein possibly implicated in higher order chromatin structure. *J. Cell Sci.* **112**, 2463-2472.
Tollervey, D., Lehtonen, H., Jansen, R., Kern, H. and Hurt, E. (1993). Temperature-sensitive mutations demonstrate roles for yeast fibrillarin in pre-rRNA processing, pre-rRNA methylation, and ribosome assembly. *Cell* **72**, 443-457.
Tong, C. G., Geichler, S., Blumenthal, S., Balk, J., Hsieh, H. L. and Roux, S. J. (1997). Light regulation of the abundance of mRNA encoding a nucleolin-like protein localized in the nucleoli of pea nuclei. *Plant Physiol.* **114**, 643-652.
Turck, N., Lefebvre, O., Gross, I., Gendry, P., Keninger, M., Simon-Assman, P. and Launay, J. F. (2006). Effect of laminin-1 on intestinal cell differentiation involves inhibition of nuclear nucleolin. *J. Cell. Physiol.* **206**, 545-555.
Uchiyama, S., Kobayashi, S., Takata, H., Ishihara, T., Hori, N., Higashi, T., Hayashihara, K., Sone, T., Higo, D., Nirasawa, T. et al. (2005). Proteome analysis of human metaphase chromosomes. *J. Biol. Chem.* **280**, 16994-17004.
Vagnarelli, P. and Earnshaw, W. C. (2004). Chromosomal passengers: the four-dimensional regulation of mitotic events. *Chromosoma* **113**, 211-222.
VandenBeldt, K. J., Barnard, R. M., Hergert, P. J., Meng, X., Maioto, H. and McEwen, B. F. (2006). Kinetochore use a novel mechanism for coordinating the dynamics of individual microtubules. *Curr. Biol.* **16**, 1217-1223.
Vandré, D. D. and Burry, R. W. (1992). Immunoelectron microscopic localization of phosphoproteins associated with the mitotic spindle. *J. Histochem. Cytochem.* **40**, 1837-1847.
Vandre, D. D., Davis, F. M., Rao, P. N. and Borisy, G. G. (1984). Phosphoproteins are components of mitotic microtubule organizing centers. *Proc. Natl. Acad. Sci. USA* **81**, 4439-4443.
Van Hooser, A., Yuh, R. and Heald, R. (2005). The perichromosomal layer. *Chromosoma* **114**, 377-388.
Wang, W., Budhu, A., Forgues, M. and Wang, X. W. (2005). Temporal and spatial control of nucleophosmin by the Ran-Crm1 complex in centrosome duplication. *Nat. Cell Biol.* **7**, 823-830.
Waters, B. A., Skibbens, R. V. and Salmon, E. D. (1996). Oscillating mitotic newt lung cell kinetochores are, on average, under tension and rarely push. *J. Cell Sci.* **109**, 2823-2831.
Yanagida, M., Shimamoto, A., Nishikawa, K., Furuichi, Y., Isobe, T. and Takahashi, N. (2001). Isolation and proteomic characterization of the major proteins of the nucleolin-binding ribonucleoprotein complexes. *Proteomics* **1**, 1390-1404.
Yanagida, M., Hayano, T., Yamauchi, Y., Shinkawa, T., Natsume, T., Isobe, T. and Takahashi, N. (2004). Human fibrillarin forms a sub-complex with splicing factor 2-associated p32, protein arginine methyltransferases, and tubulins alpha3 and beta1 that is independent of its association with preribosomal ribonucleoprotein complexes. *J. Biol. Chem.* **279**, 1607-1614.
Yuan, X. J., Zhou, Y. G., Casanova, E., Chai, M. Q., Kiss, E., Grone, H., Schutz, G. and Grummt, I. (2005). Genetic inactivation of the transcription factor TIF-IA leads to nucleolar disruption, cell cycle arrest, and p53-mediated apoptosis. *Mol. Cell* **19**, 77-87.
Zatsepina, O. V., Rousselet, A., Chan, P. K., Olson, M. O. J., Jordan, E. G. and Bornens, M. (1999). The nucleolar phosphorylation B23 redistributes in part to the spindle poles during mitosis. *J. Cell Sci.* **112**, 455-466.

Journal of Cell Science